

## Phase composition and residual stresses in thermal barrier coatings

A A Lozovan<sup>1</sup>, S Ya Betsofen<sup>1</sup>, A A Ashmarin<sup>2</sup>, B V Ryabenko<sup>3</sup> and S V Ivanova<sup>4</sup>

<sup>1</sup> Moscow Aviation Institute (National Research University), ul. Orshanskaya 3, Moscow, 121552, Russia

<sup>2</sup> Institute of Metallurgy and Materials n. a. A A Baykova, Russian Academy of Sciences, Leninsky pr. 49, Moscow, 119991, Russia

<sup>3</sup> FGUP NPTsG Salyut, Moscow, 105118, Russia

<sup>4</sup> National Research Nuclear University MEPhI (Moscow Engineering Physics Institute), Moscow, 115409, Russia

E-mail: loz-plasma@yandex.ru

**Abstract.** X-ray study of the phase composition and residual stresses distribution in two-layer APS coatings showed that the ceramic layer consists of  $t$ -ZrO<sub>2</sub> phase with tetragonal lattice and the metal underlayer  $\gamma$ -solid solution based on nickel. In the transition zone thickness of  $\sim 100$   $\mu$ m as the distance from the surface was revealed a gradual transition from  $t$ -ZrO<sub>2</sub> to  $\gamma$ -solid solution. Increase in the specific volume of the metal underlayer resulting TGO growing leads to the formation of this layer high compressive stresses up to 600 MPa. In this case, the ceramic layer contains tensile stress up to 200 MPa.

### 1. Introduction

The studies performed in the last two decades in this field were directed toward improvement of the structure and properties of coatings with a ZrO<sub>2</sub> based external ceramic layer, which decrease the substrate material temperature by 100–150 °C [1, 2]. Alloying of ceramic with 7–8 wt. % Y<sub>2</sub>O<sub>3</sub> stabilized the tetragonal modification of ZrO<sub>2</sub> and provided the formation of the  $t'$  phase, which is stable within several hundred thermal cycles in the temperature range up to 1200 °C. The resource of TBC depends substantially on the residual stresses, which are very high at the boundary between a ceramic layer and the metallic sublayer. It mainly consists of thermal growing oxide (TGO) Al<sub>2</sub>O<sub>3</sub>, which is the product of oxidation of a metallic MCrAlY sublayer. The purpose of this work is to study the distribution of phase composition, structure, and residual stresses in TBC by X-ray diffraction, scanning electron microscopy, and electron-probe microanalysis of the chemical composition in coating layers.

### 2. Experimental

Multilayer TBCs were deposited onto an ZhS26 alloy substrate in the following sequence: a metallic sublayer, a gradient (metal ceramic) intermediate layer, and a basic (external) ceramic layer. The external ceramic layer, the intermediate gradient layer, and the part of the metallic sublayer adjacent to it were deposited by plasma spraying in air in an automatic UniCoat (Sulzer Metco) device. The phase composition and the residual stresses in TBC were studied by X-ray diffraction (XRD) using a vertical



XRD-6000 SIMADZU device and  $\text{CuK}_\alpha$  radiation (wavelength  $\lambda = 0.154178$  nm). Crystalline phases were identified using the ICDD-2003 database.

### 3. Results and discussion

The X-ray diffraction pattern of the surface layer in the coating consists of lines of the tetragonal phase and only traces of the monoclinic phase (figure 1). This phase composition is retained to a depth of 180  $\mu\text{m}$ . The X-ray diffraction patterns of the coating layers at a depth of 200–270  $\mu\text{m}$  from the surface contain the lines of two phases, namely,  $t\text{-ZrO}_2$  with yttria and an FCC nickel-based  $\gamma$ -solid solution (figure 2). This part of the coating corresponds to the intermediate gradient layer. The  $t\text{-ZrO}_2$  phase is predominant in the part of the layer adjacent to the ceramic layer (figures 2(a), 2(b)), and a nickel-based  $\gamma$ -solid solution with an FCC lattice parameter  $a = 0.358\text{--}0.359$  nm is predominant in the part next to the metallic sublayer (figure 2(d)). Note the presence of a satellite line near the (111) line of the  $\gamma$ -solid solution in all X-ray diffraction patterns of the intermediate layer. It can be attributed to an analogous line from pure nickel with  $a = 0.352$  nm or to the (110) reflection of the  $\beta$ -phase (NiAl with the B2 lattice).

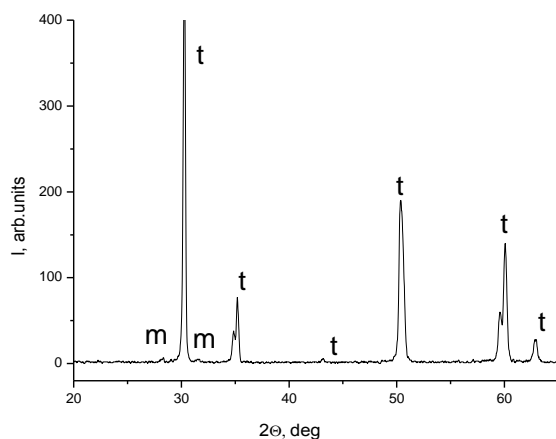


**Figure 1.** X-ray diffraction pattern of the surface of the ceramic layer.

The presence of the  $\beta$ -phase in this layer is possible, since the  $\gamma$ -solid solution in the intermediate layer adjacent to the external ceramic layer has the higher aluminum content as compared to the metallic sublayer. However, the (200) reflection of this phase (which has the highest intensity) is absent in all X-ray diffraction patterns of the metal ceramic layer that contain the satellite line, and the position of this line could correspond to the (110) reflection of the  $\beta$ -phase (see figures 2(b), 2(c)). Since the line intensities of the  $\gamma$ -solid solution indicate the absence of a pronounced texture, it is unlikely that the  $\beta$ -phase has such a strong texture that even traces of the most intense reflection are absent in an X-ray diffraction pattern. Thus, this satellite line should be attributed to a  $\gamma$ -solid solution depleted of alloying elements with a lattice parameter close to that of pure nickel. The presence of this line indicates that the oxidation of the  $\gamma$ -phase with the formation of TGO ( $\text{Al}_2\text{O}_3$ ) begins at the stage of coating deposition. The oxidation of the  $\gamma$ -phase proceeds selectively, by the extraction of aluminum from the  $\gamma$ -solid solution. This is accompanied by the aluminum depletion of the  $\gamma$ -solid solution, at decrease in the lattice parameter from 0.359 to 0.352 nm, and the formation of  $\text{Al}_2\text{O}_3$  in the intermediate layer next to ceramic. This behavior is reflected in X-ray diffraction patterns in the form of the satellite line near the main reflection of the  $\gamma$ -solid solution at an angle  $2\theta \approx 44^\circ$ , which is shifted toward high angles ( $2\theta \approx 45^\circ$ ) from this reflection (see figures 2(b)–2(d)). The results of layer-by-layer analysis are generalized as the TBC (except for the ceramic layer) depth profiles of the lattice parameter of the nickel solid solution (figure 3). These results support the idea of the structural scheme of TBC, where a gradient metal ceramic layer forms between the metallic sublayer and the external ceramic layer. This gradient layer forms upon spraying of a  $\text{ZrO}_2\text{--}8\text{Y}_2\text{O}_3$  ceramic powder preliminarily clad by nickel and aluminized. The intermediate layer is characterized by higher lattice parameters as

compared to the metallic sublayer. This finding points to a higher aluminum concentration in the intermediate layer, which should increase the heat resistance of TBC and its service life. The most important role of the gradient layer is likely to be the fact that metal oxidation with the formation of TGO occurs in this layer, where metallic component particles are located discretely rather than forming extended layers. In the absence of the gradient layer, TGO forms at the interface between the ceramic and the metallic sublayer in the form of a continuous interlayer, which leads to the separation of ceramic when TGO reaches the critical thickness. Therefore, in the presence of the gradient intermediate layer, TBC fails significantly later and the service life of the structure increases.

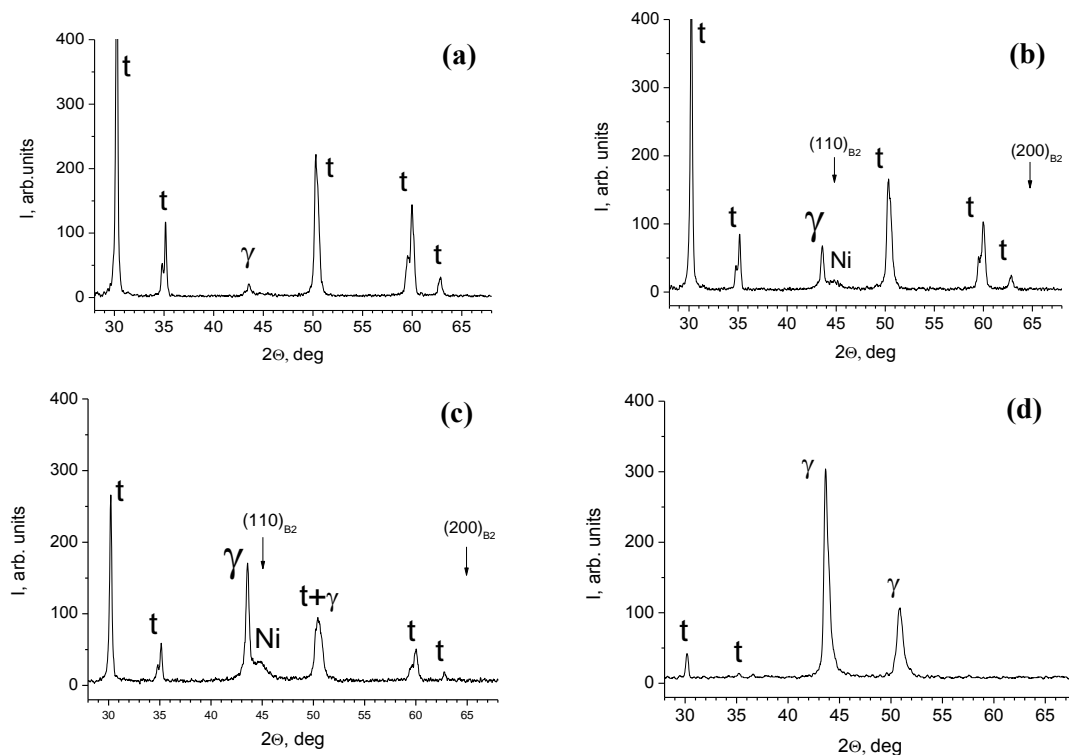


**Figure 2.** X-ray diffraction patterns of the layers in TBC that are located between the ceramic layer and the metallic sublayer at a distance from the coating surface, mm: (a) – 0.2; (b) – 0.22; (c) – 0.24; (d) – 0.27.

The process of coating deposition implies a nonuniform composition across the coating thickness and, hence, a lattice parameter gradient. Therefore, the  $\sin^2\psi$  method becomes ineffective to determine the residual stresses. Figure 3 shows how the lattice parameter of solid solution changes with depth. The conditions of recording X-ray diffraction patterns in the  $\sin^2\psi$  method are such that the lattice parameter gradient introduces substantial errors in the determination of the residual stresses. Therefore, to determine the residual stresses, we propose to use the technique [3], which allows us to avoid the errors related to the variation of the lattice parameter across the surface layer thickness. This technique is based on measuring the interplanar spacings for reflections  $(h_1k_1l_1)$  and  $(h_2k_2l_2)$ , which exhibit the strongest difference between the elastic constants.

For cubic and tetragonal crystals, the residual stress is calculated from the relationship:

$$\sigma_{res} = \frac{a_{h_1k_1l_1} - a_{h_2k_2l_2}}{2(a_{h_2k_2l_2} K_{h_1k_1l_1} - a_{h_1k_1l_1} K_{h_2k_2l_2})}, \quad (1)$$

where  $a_{h_1k_1l_1}$  and  $a_{h_2k_2l_2}$  are the lattice parameters determined from the interplanar spacings for reflections  $(h_1k_1l_1)$  and  $(h_2k_2l_2)$ .

Elastic constants  $K_{hkl} = (\nu/E)_{hkl}$  are calculated using equations (2) and (3), respectively, for the cubic and tetragonal crystals:

$$\left(\frac{\nu}{E}\right)_{hkl} = -s_{11} - (s_{11} - s_{12} - 0.5s_{44})(h^2k^2 + h^2l^2 + k^2l^2) / (h^2 + k^2 + l^2), \quad (2)$$

$$\left(\frac{\nu}{E}\right)_{hkl} = s_{11}(h^2l^2 + k^2l^2 + 2h^2k^2) + (s_{33} - s_{44})(h^2l^2 + k^2l^2) + s_{12}(h^4 + k^4 + h^2l^2 + k^2l^2). \quad (3)$$

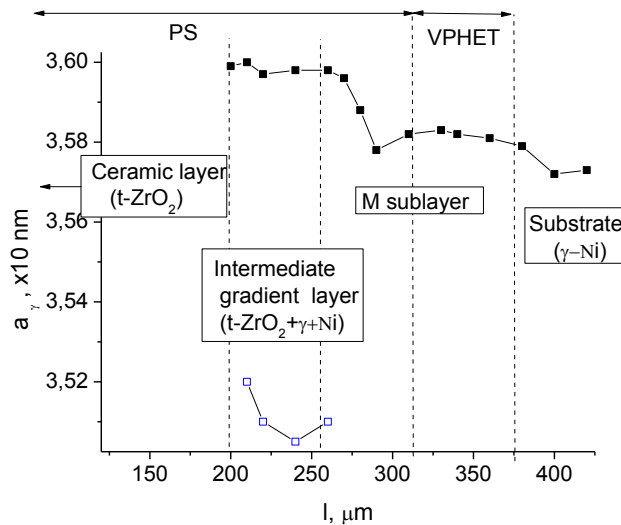


**Figure 3.** Depth profile of the lattice parameter of the  $\gamma$ -solid solution across TBC. PS is plasma spraying, and VPHE is vacuum plasma high-energy technology.

It is well known that sequential removal of surface layers occur relaxation of residual stresses which must be considered [4]. If the surface layer contains residual stresses, e. g. tensile stresses, they affect the remaining cross section of the sample via their axial and bending components, which are compensated by the axial stresses and moments of the opposite sign in the remaining cross section of the sample. Therefore, layer removal changes the stress distribution in the remaining part of the sample. When a layer of thickness  $a$  is etched off, the relaxed stresses are found by the summation of the stresses for all of the layers removed earlier. The stress in the removed layer ( $\Delta\sigma_a$ ) of thickness  $a$  can be obtained by summation over all sequentially removed layers  $\Delta x_i$ :

$$\Delta\sigma_a = \sum \left[ \Delta x_i \frac{\sigma_{i-1} + \sigma_i}{2} \left( \frac{1}{h-x_i} + 3 \frac{h-x_i + \Delta x_i}{(h-a)^2} \right) \right].$$

The stress in a layer located at a distance  $a$  from the surface is then determined by the relation:

$$\sigma_a = \sigma^{meas} - \Delta\sigma_a.$$

Figure 4 shows the distribution of the experimental ( $\sigma^{meas}$ ) and adjusted ( $\sigma_a$ ) values of residual stresses over the entire cross section of TBC. According to these data, compressive stresses (600 MPa) are only present in the metallic sublayer, which is likely to be related to the formation of  $Al_2O_3$  (which occupies larger atomic volume as compared to the metal). Peak tensile stresses are shifted by 50–100  $\mu m$  from the ceramic layer to the gradient layer, i. e. from brittle ceramic to a more ductile metal ceramic. Stresses are absent in a significant part of the ceramic layer (figure 4).

#### 4. Conclusions

An X-ray method of determining residual stresses based on the features of elastic anisotropy of the elastic characteristics of the ceramic and metal components of the TBC.

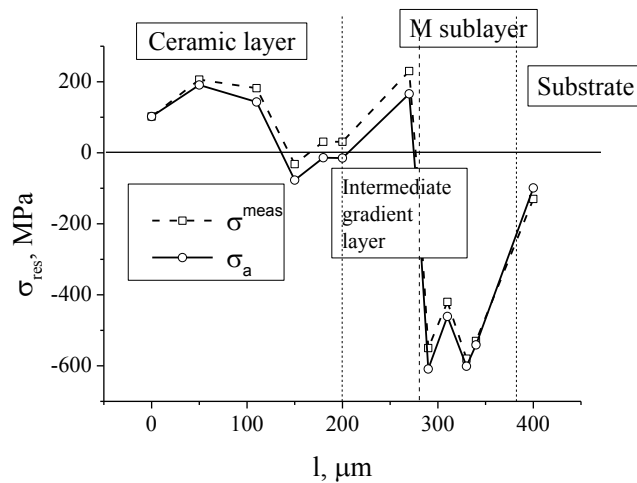


**Figure 4.** Distribution of residual stresses across TBC. PS is plasma spraying, and VPHET is vacuum plasma high-energy technology.

We proposed a technique for the correction of the residual stresses measured by an X-ray method along the depth of a coating with allowance for their relaxation upon the removal of surface layers.

The effectiveness of techniques demonstrated by TBC, consisting of a ceramic outer layer  $\text{ZrO}_2\text{--}8\text{Y}_2\text{O}_3$  and the metal underlayer of an alloy NiCrAlY.

It is shown that the outer ceramic layer formed tensile stresses reach values of 200 MPa, which are likely the origin of quench, thus forming a metallic underlayer compressive stresses which reach 600 MPa, which are associated with an increase in specific volume due to the formation TGO.

### Acknowledgments

The study was performed by a grant from the Russian Science Foundation (project №15-19-00241).

### References

- [1] Cernuschi F, Bianchi P, Leoni M and Scardi P 1999 *J. Therm. Spray Technol.* **1** 102
- [2] DeMasi-Marcin J T and Gupta D K 1994 *Surf. Coat. Technol.* **68–9** 1
- [3] Betsofen S Ya, Bannykh I O and Sarychev S M 2006 *Russian Metallurgy (Metally)* **5** 385
- [4] Betsofen S Ya, Plikhunov V V and Ashmarin A A 2008 *Russian Metallurgy (Metally)* **2** 148